NOTCH SIZE EFFECT ON FATIGUE PERFORMANCE OF DUCTILE IRON

F.S. Ahmed
Shoubra Faculty of Engineering,
Zagazig University, Cairo, Egypt.

ABSTRACT

The effect of notch size on fatigue behaviour of ductile iron (DI) was experimentally determined. Rotating bending high-cycle fatigue data were obtained for pearlitic and ferritic DI_s in the notched and unnotched conditions. Behaviour of DI specimens containing long cracks was obtained from compact tension (CT) specimens of 25mm thick.; the crack propagation rate da/dN and threshold stress intensity factor range ΔK_{th} were determined, in accordance with the ASTM-E647(88) standard specifications. By combining the fatigue limit data of smooth surface specimens σ_e and the threshold value of stress intensity ΔK_{th}, obtained from conventional fracture mechanics, CT specimens, a plot of the Kitagawa-Takahashi type was constructed to define the effect of crack size on the safe working fatigue stress, for both pearlitic and ferritic DI_s. Plot data, besides scanning electron microscopic (SEM) investigations of the fractured, unnotched fatigue specimen surfaces revealed clearly that fatigue cracks have been originated at regions containing metallurgical defects, involving sizes in the range 50-90 μm. The harmful effect of these defects comes from the inherently three dimensional nature. Size of these defects is, therefore, considered to represent a lower bound of surface roughness. Results,also, indicated that machining (surface) defects responsible for crack initiation are in the order of or greater than the largest present metallurgical defect. Consequently; surface quality impovement by super finishing processes, will not have a measurable effect on the bending fatigue strength of DI. Beyond 250 μm of surface defects, the fatigue limit of pearlitic DI has shown to decrease by increasing the severity of notch and, at notch depth > 1.5mm., linear elastic fracture mechanics (LEFM) predictions become too conservative. Finally plots relating the applied stress range ($Y\ \Delta\sigma$) and initial flaw size,a_i, were constructed for definite numbers of cycles; these plots help in forecasting the fatigue life of large section DI components containing pre-specified defects. They,also, showed that longer cyclic life can be realized by decreasing the initial flaw size than by increasing plane strain fracture toughness and, the use of ferritic DI provides longer fatigue life, as ferritic matrix can decrease the crack growth rate and tolerate the critical defect size to a greater extent.

NOMENCLATURE

a	crack length
a_o	material constant
da/dN	crack growth rate
A,n	crack propagation material constants
ΔK	stress intensity range
ΔK_{th}	threshold stress intensity range
K_{1c}	plane strain fracture toughness
N	number of cycles
R	ratio of minimum stress to maximum stress
$\Delta\sigma$	stress range
σ_e	fatigue limit
Y	crack geometry factor

INTRODUCTION

Ductile irons (DI_s) are being increasingly used in highly stressed components, particularly in the automotive industry. Therefore, it becomes essential to thoroughly understand the factors influencing the fatigue properties of these materials. It is well known that surface condition has a strong effect on fatigue life, also, metallurgical impurities, e.g. enlarged graphite nodules and shrinkage pores are considered preferential sites for fatigue crack initiation (1-7).

The effect of defect (crack) size on the fatigue strength can be conveniently described by means of the so called kitagawa -Takahashi plot (1,2and 7-15), relating the crack fatigue stress range,$\Delta\sigma$, with the

crack size, a, in a logarithmic scale, as shown in Figure (1). In this plot, the crack length axis is divided into three regimes, according to crack performance under the applied loads:

1- The microstructuray short crack (MSC) regime, in which the crack length, a, is of the same order of magnitude as metallurgical features (zone I in the Figure). These are not dangerous cracks and, below a certain size MSC has no effect on the fatigue limit at all.

2- The physically short crack (PSC) regime (zone II), which involves crack sizes in the range 50-500 μm. For these cracks, very unusual behaviour has been reported by a number of investigators (1,5 and 5-13) who showed that, the crack growth rate tended to decelerate at increasing crack length and that eventually the crack stopped when the specimen was tested below the endurance limit. These cracks have been observed to exhibit equal or greater propagation rates than those corresponding to long cracks, subjected to the same nominal stress intensity factor range ΔK. Many theories have been developed (5,9,12 and 13) to account for the effect of short cracks on fatigue behaviour. The most simple form is given by El Haddad, in which a simple expression is used to characterize the variation of fatigue limit with crack length

$$\Delta K = \Delta\sigma\sqrt{\pi(a+a_o)} \qquad (12 \text{ and } 13)$$

where, a, is the actual crack length and when ,a, approaches zero

$$a_o = \frac{1}{\pi}.\left(\frac{\Delta K_{th}}{\Delta\sigma_e}\right)$$

where ΔK_{th} = threshold stress intensity factor range, determined from long cracked test-specimens ($a >> ao$).

$\Delta\sigma_e$ = endurance limit for unnotched samples.

ao is a material property, it represents the effective crack length at which the fatigue limit stress will just propagate a crack into the interior of the material.

3- Long crack regime (zone III); in which the crack length a > 0.5mm, and when the crack tip plasticity is minimal (crack propagating at a low stress level). A quantitative evaluation of the load-bearing capacities of engineering compo... containing large cracks has been developed, ... the linear elastic fracture mechanics (LE... approach. This relates the stress intensity fact... the applied stress range $\Delta\sigma$ and the crack len... in the form

$$K = Y\Delta\sigma\sqrt{\pi a}$$

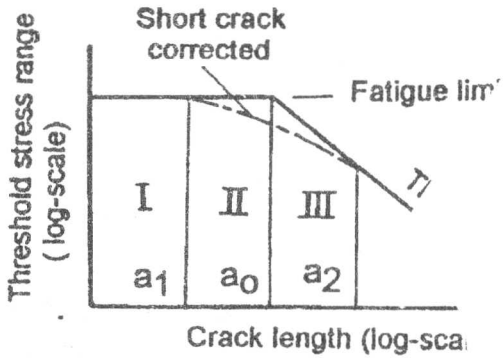

Figure 1. Sxchematic kitagawa plot for behaviour.

where Y is the crack geometry factor. Th... stress intensity factor range, ΔK_{th}, represents operating limit, below which fatigue damage ... unlikely. It is extremely important in engi... applications to evaluate the critical crack length ... the figure), in order to decide whether the gr... characteristics of long cracks (LEFM) can be used ... the prediction of remaining fatigue life when s... defects or small cracks are detected in se... conditions.

- In many situations the avoidance of catastro... failure depends not only on a knowledge of ... conditions necessary for fast fracture or coll... but, also, on the ability to predict the rate of gr... of existing sub-critical defects. Therefore, it ... the highest important that, reliable methods ... established for determining the rate of growth ... pre-existing defects. In fracture mecha... terminology, the crack-growth rate has ... described by several equations, but the si... Paris-Erdogan power law:

$$da/dN = A(\Delta K)^n$$

still remains the popular form (3,5 and 25-28) and

will be assumed adequate for purposes of this paper. In this equation da/dN is the crack propagation per cycle, ΔK is the stress intensity range and, A and n are material constants. The substitution of equation (1) into equation (2), followed by integration gives the equation for cycles to failure, N_f, with the starting and final flaw sizes as limits of the integration. When the geometrical correction factor, Y, does not changed within the limits of integration and, for those situations where $n \neq 2$, the cyclic life is given by :

$$N_f = \frac{1}{A.(Y\Delta\sigma)^n.\pi^{n/2}.(1-n/2)}\left(\frac{1}{a_f^{n/2-1}} - \frac{1}{a_i^{n/2-1}}\right) \quad (3)$$

The critical crack size indicating that single cycle fracture is approached, $A_f = \frac{1}{\pi}.(\frac{K_{1c}}{\sigma_e})^2$ is used as the upper limit of integration, while the lower limit indicates that zero crack growth is approached and, the threshold value of stress intensity, ΔK_{th} is used. The initial defect size, a_i, represents a pre-existing value for which the fatigue number of cycles is determined.

- Present work:

Review of literature indicated that insufficient work has been done to establish fatigue crack growth rate in DI, also, in spite of the great volume of work done on the high-cycle fatigue performance of notched DI specimens, no reliable quantitative models have been developed to describe the effect of surface roughness and casting defects on the safe working fatigue stress, as well as, fatigue life of DI components. Therefore, this study relies upon a large experimental program, in which, fatigue behaviour of DI test specimens, containing MSC, PSC and long cracks were studied. DI in the as cast or pearlitic (PDI) and annealed or ferritic (FDI) conditions, were used in this investigation and, the obtained data were used to construct the Kitagawa-Takahashi plot. In order to relate the fatigue initiation sites, with specimen defects; scanning electron microscope was used to examine the failed surfaces of test specimens. Finally, diagrams were constructed, relating the applied stress range ($Y\Delta\sigma$) and initial defect size, a_i, which help in forecasting the fatigue life of PDI and FDI large section components, containing pre-specified sharp defects.

Experimental technique

The DI used in the experiments, was produced by the way described in a previous study (29). The chemical composition wt% was: C 2.96, Si 2.31, Mn 0.25, P 0.02, S 0.011, Mg 0.043 and remainder Fe. The microstructure of 35-40% pearlite, nodule count of 250-300 nodules/squ.mm, nodule size in the range of 10-30 mm and nodularity in excess of 95%, is shown in the photo-micrographe of Figure (2). The material also, contained a number of enlarged nodules and micro-shrinkage pores, however, these defects were rather scarce. Mechanical properties of PDI are : tensile strength = 610 MPa, ductility = 9% and Brinell hardness number 220. Annealing was performed at 750°C for 7 hours and furnace cooling. Mechanical properties of FDI are: tensile strength = 280 MPa and ductility = 21%.

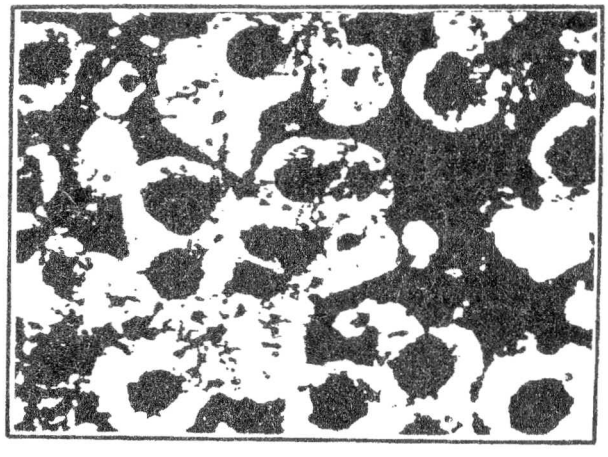

Figure 2. As cast ductile peartitic iron x 400.

A- Fatigue test

Fatigue tests were performed on a specially designed, rotating bending fatigue testing machine (30). Geometry and dimensions of the fatigue test specimen are shown in Figure (3-a). Specimens are mounted as cantilevers and tested at a stress ratio R=-1, frequency of 21 Hz and a wide range of stress amplitudes. At least three specimens were tested for each stress level, the number of cycles to failure were recorded and, the fatigue limit was evaluated at $3X10^6$ cycles. All tests

are conducted at room temperature, in laboratory air.

In order to cover a range of surface roughness, the test section of specimens was subjected to different grades of surface finish, using the following methods:

a- Polishing, using hand polishing in the circumferential direction at graded levels to 1 μm diamond paste.

b- Grinding, using the 200 grade emery paper.

c- Rough turning with a tungsten carbide tool.

d- Fine turning and, a series of regular grooves were then produced in the circumferential direction, by repeated passes of the turning tool (see Fig. 3-b). A series of three V-grooves, equally spaced with one millimeter pitch, were made along the central gauge length of the test specimens, details of the notch profile are indicated in Fig. (3-c). Two different roughness levels were produced by this method: 0.25 and 0.5 mm. deep with 90° included angle.

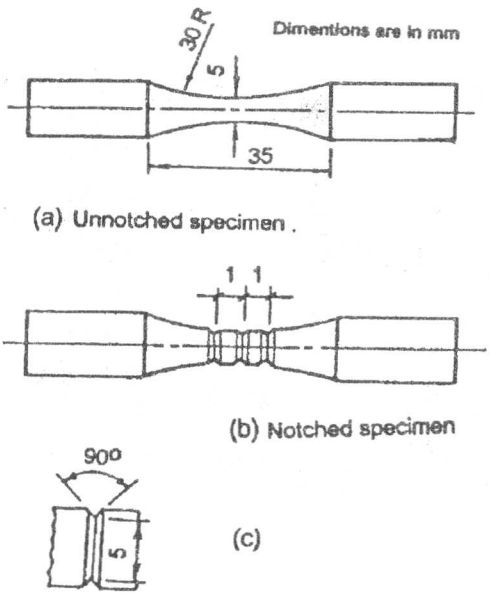

Figure 3. Fatigue test specimen configurations.

Surface roughness measurements

Two measures of roughness were produced, the standard center-line average R_a, generated automatically by the Talysurf and, the maximum pit depth denoted R_{max}, and defined as the depth of the largest pit, recorded on a 4mms length of the surface. All stylus traces were taken parallel to the specimen axis, in the maximum stress region, where all cra initiation was found to takes place. As it was expecte vacancies of the surface graphite nodules, promot surface roughness measures, especially the R_m values. The Table indicates results of Talysurf traces the tested specimen groups.

Surface Roughness Data

Condition	$R_a(\mu m)$	$R_{max}(\mu m)$
Polished	0.3-0.7	10 - 15
Coarse ground	1-3	20 - 30
Rough turning	70-75	103-110
Small groove	-	250-265
Large groove	-	500-520

All of the specimen types were tested in the machined conditions, without any attempt to allevia surface residual stresses introduced by the machinin processes, as stress relief treatment may alter th metallurgical conditions of the materials.

- Scanning electron microscope (SEM) was used t examine the failed surfaces of test specimens, order to relate the fatigue initiation sites t specimen defects.

B- Fatigue threshold (ΔK_{th}) and crack propagation rat (da/dN)

In order to determine the crack growth rate, da/dN as well as threshold stress intensity factor range, ΔK_{th} CT specimens of 25 mms thickness and proportions a indicated in Figure (4), were put into a specially designed Push-Pull fatigue testing machine, as shown in Figure (5). The main idea of the machine i indicated in the appendix. Specimens were fatigue precracked, then subjected to pre-specified cyclic loading at a stress ratio R= -1 and frequency of 1 Hz. Tests were performed at three levels of loading amplitudes, namely S_a=18, 21 and 24 KN. The crack length is measured as a function of elapsed fatigue cycles. The threshold stress intensity factor range, ΔK_{th}, was determined by shedding technique, a value of 5% decrease in load at each step was employed. Tests were conducted in laboratory air, according to the ASTM-E647(88) standard specifications (31).

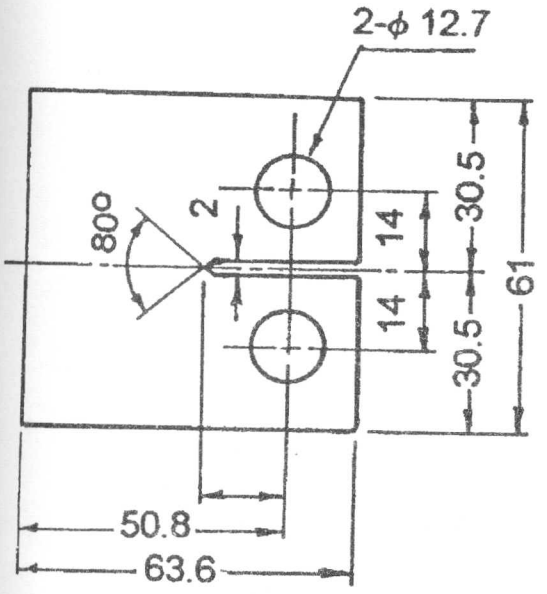

Figure 4. Dimensions of compct tension specimen.

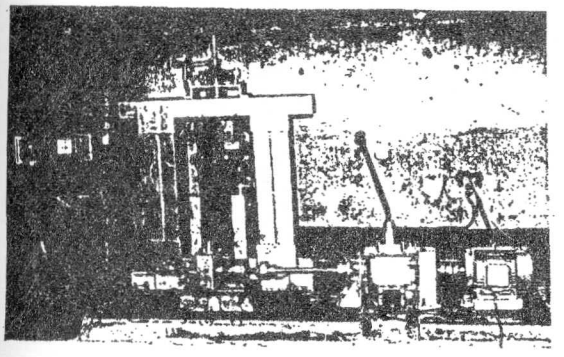

Figure 5. Setup for fatigue crack propagation.

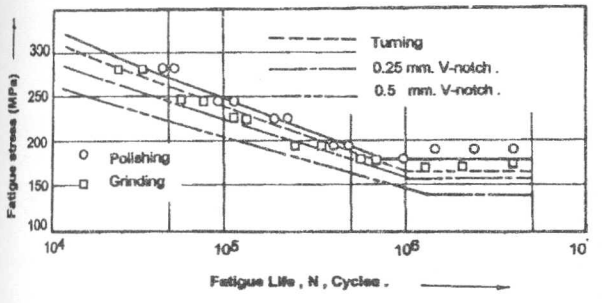

Figure 6. S-N Diagrams for notched & unnotched FDI specimens.

RESULTS

The S-N diagrams, obtained for the all machining conditions of PDI and FDI are indicated in Figures (6) and (7), respectively. Curves are established using the method described in the ASTM - E739(80) standard specifications(32). It may be observed that surface roughness affects the fatigue limit of PDI to a higher degree and, presence of 0.5mm. deep V-notch, reduces the fatigue limit to a greater extent.

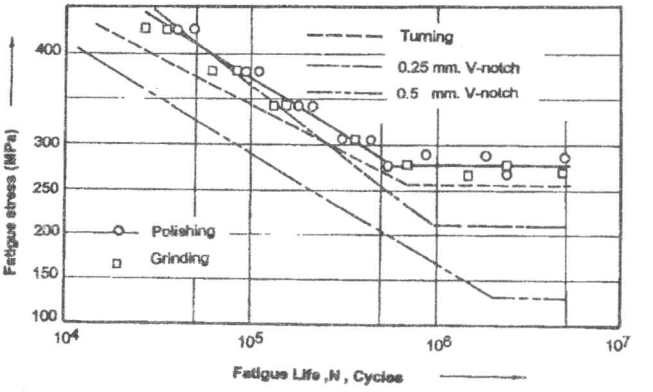

Figure 7. S-N Diagrams for notched & unnotched PDI specimens.

Figure (8) shows some photo-micro graphs, obtained by SEM for the fractured surfaces of notched and unnotched fatigue test specimens. Figure (8-a) indicates clearly that fatigue cracks had initiated in the root of machined notch. The white area in Figure (8-b) represents a micro shrinkage pore of about 50 μm size, acting as initial site for critical crack. Generally, rough textures were observed for all the investigated fractured surfaces, stepped faces were, also, found as shown in Figures (8-b and c).

The dependence of the macroscopic crack growth rates da/dN, measured on CT specimens on the ΔK-value is shown in Figures (9-a and b) for both, PDI and FDI ; the two Figures are very similar. The crack growth rates were obtained by drawing tangents to the curves relating the crack length and number of cycles, then a numerical analysis was performed to establish the crack growth rates. In the interest of design safety, it is prudent to use a well-established method of statistical analysis to determine constants of the crack growth rate equations. The method of least square with plus two standard deviations on da/dN was used here and resulted, under the K_{max} - constant test conditions, in the following equations:

$$da/dN = 4.16 \times 10^{-12} (\Delta K)^{5.32} \quad \text{for PDI \&}$$
$$da/dN = 8.85 \times 10^{-11} (\Delta K)^{4.58} \quad \text{for FDI}$$

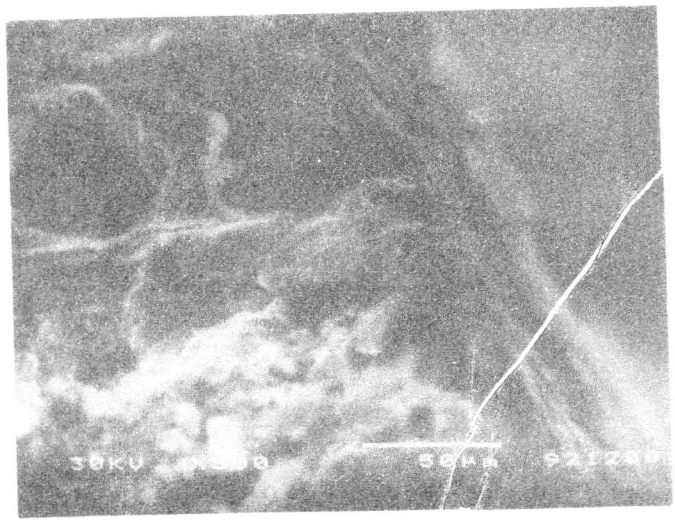

(a) Typical machining tear responsible for crack initiation in a v-grooved test specimen.

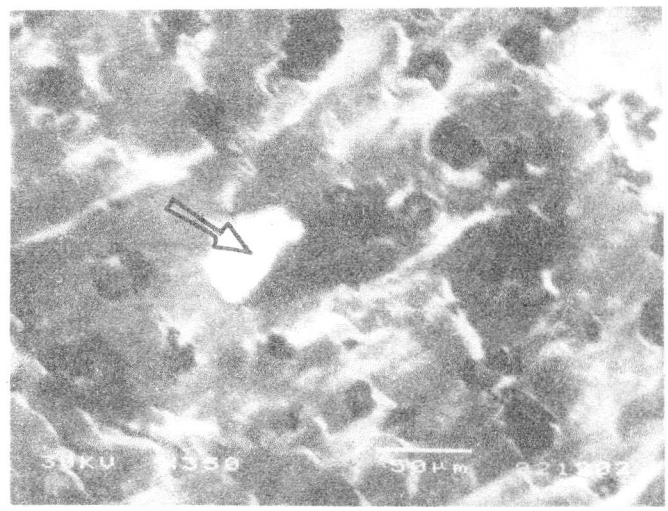

(b) A pore of about 50 μm acting as initial site for critical crack.

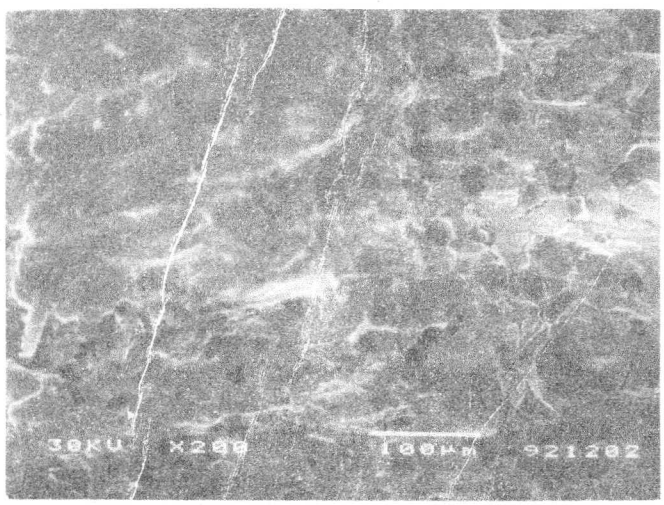

(c) Stepped fracture indicating crack branching or multiple initiation sites.

Figure (8) Fracture morphologies obtained by SEM for (a) notched and (b&c) unnotched fatigue test specimens.

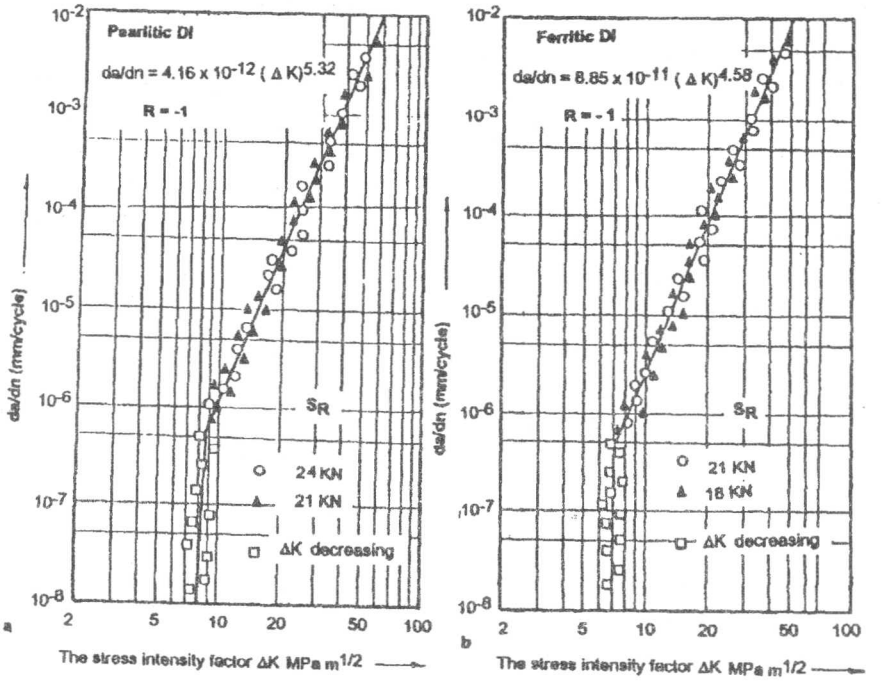

Figure 9. Fatigue crach growth rate as a function of stress intensity factor range ΔK for Pearlitic Dl & Ferritic Dl.

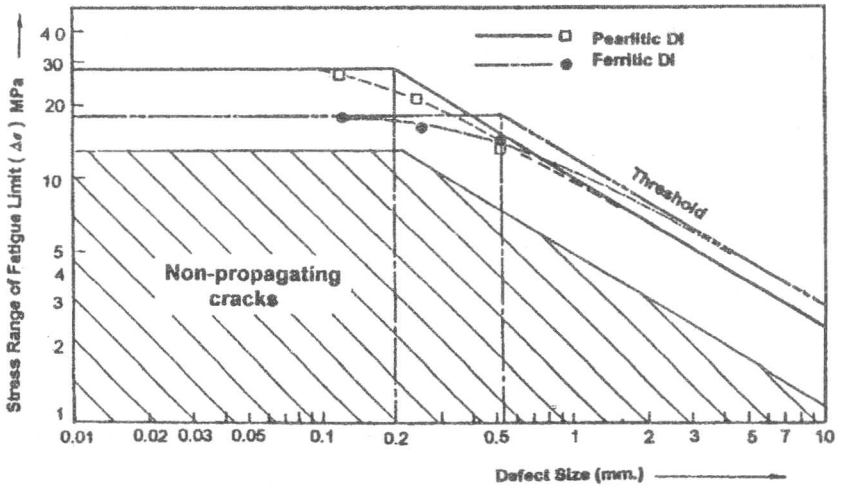

Figure 10. Dependence on crack size of the fatigue limit: Kitagawa-Takahashi diagrams for Pearlitic Dl and Ferritic Dl.

The units on da/dN are mms per cycle and Δ K are MPa.$m^{1/2}$. Threshold values of 8 MPa.$m^{1/2}$ and 7 MPa.$m^{1/2}$ were obtained under ΔK decreasing test conditions for PDI and FDI respectively.

By combining the fatigue limit data of smooth surface specimens σ_e and the ΔK_{th} data from conventional fracture mechanics CT specimens, it is possible to construct the diagram defining the effect of crack depth (defect size) on the safe working fatigue limit. This diagram is shown in Figure (10) where, the maximum pit depth, R_{max} was plotted against endurance limit in a logarithmic plot of the Kitagawa-Takahashi type. In

this diagram the fatigue limit of polished specimens, σ_e, appears as a horizontal line and, the crack threshold, ΔK_{th}, appears as straight line of slope $= -\frac{1}{2}$, (since $\Delta K \propto \frac{1}{\sqrt{a}}$) at an intersection point of $R_{max} = a_o$. A value of a_o=0.2mm was obtained for PDI and, a larger value of 0.5 mm. was deduced for FDI. The fatigue limits of specimens containing V-notches, or PSC were plotted ,also. It can be observed that, present data of the V-notched specimens fall close to the intersection point of the two straight lines, almost all points inhabit the region below the intersection points.

The graphical presentation of Equation (3), for the determination of the fatigue number of cycles of component containing defects, is shown in Figures. (11) & (12) for PDI and FDI respectively. The cyclic stress range ($Y.\Delta\sigma$) is plotted against initial flaw size, a_i. The critical crack size for single cycle fracture A_f $[A_f = \frac{1}{\pi}.(\frac{K_{1c}}{\sigma_e})^2]$ is used as the upper limit of integration and, the lower limit is defined by the threshold values. The lines between these two extreme boundaries represent constant cyclic lives, as labeled; these are asymptotically approached to the critical crack sizes, A_f, as indicated in the Figures. It should be noted that, the plane strain fracture toughness (K_{1c}), used in the determination of critical crack size, A_f, for PDI was determined in a previous study (33), and has a value of 70 MPa $m^{1/2}$. The calculated critical crack size A_f = 4.2 mms. Whereas, for FDI, it is more difficult to evaluate the critical defect size, in accordance with conventional ASTM requirements. The inherent toughness and ductility do not permit a sufficient constraint condition at the crack tip of CT specimens, so as to attain valid K_{1c} measurements. However, a valid K_{1c} value was determined, in a previous work (34) by using the double torsion test procedure and, a value of K_{1c}=40 MPa $m^{1/2}$ was obtained. Introducing this value, the evaluated critical defect size was A_f =12.7 mms. On the other hand, published data (3), based on elastic-plastic and post-yielding fracture mechanics, indicated that the critical defect size for FDI is certainly greater than 12mms. Therefore a value of A_f =12.7 mms was introduced into equation of cyclic fatigue life.

DISCUSSION

The obtained S-N diagrams indicated that s roughness is effective in reducing fatigue life and, FDI is relatively insensitive to surface roug Notch brittleness is, therefore, likely to be evident in the higher strength DI, as notch sens of the harder pearlitic structure is obviously than that of ferritic ones. On the other hand, res PDI indicated that there is no significant differe fatigue limits of the coarse ground and po specimens. SEM inspection of the failed spe surfaces revealed that, fatigue cracks in specimens originated either from over-size nodul micro-shrinkage pores as shown in Figure Fatigue crack propagation zone always appear rather rough, sometimes difficult to distinguish the fast fracture zone, also, steps were often prese the fracture faces (Figures. (8-b and c)), indic crack branching and/or multiple crack initiation Whereas, examination of the fractured faces o failed notched specimens showed that, crack initi invariably occurred at the root of circumfer notches, as indicated in the SEM micro grap Figure (8-a).

In DI the cohesion between graphite nodules and ferritic matrix is low and nodules are, therefore, as holes. As nodule size decreases this effe reduced. The harmful effect of over-size nodule well as metallurgical impurities and micro shri pores comes from the inherently three-dimens nature of these defects, although SEM data re only the situations observed from surface inspec Presence of sharp edges increases the dangers of defects to a greater extent. Therefore, it ma concluded that MSC size represents a limiting bound for the surface roughness, or maximum depth, produced by the machining operations improving the quality of the surface by lap honing, polishing or fine grinding will not ha measurable effect on the bending fatigue Generally, it was found that depths of machi defects responsible for crack initiation are in the o of, or greater than the maximum size of the pre metallurgical defects, i.e. if the machining of a sur provides surface indentations greater than maximum size of present metallurgical defects, sur cracks are originated and fatigue life would decreased

Verifications of the above conclusion have been promoted by the Kitagawa-plot (Figure (10)), which indicated that surface cracks in the order of 100 μm, represents an upper bound of surface roughness ,R_{max}, for non-propagating cracks. Larger surface roughness are, therefore, acting as crack initiation sites and, reducing the endurance limit. SEM investigations on the fractured surfaces of these specimens, revealed that the maximum size of metallurgical defects was in the order of 50-90 μm. The plot also, indicated that surface cracks larger than 1.5mm (a_2), are considered as long cracks in PDI and LFEM approach is applied, this value represents the upper limit to the use of PSC approaches. For FDI a higher value of the limiting crack length for PSC regime (a_2), is obtained ($a_2 > 3$ mms), this is attributed to the inherent ductility of ferritic structure, as it affects the crack tip stress state.

Applying a suitable safety factor to the Kitagawa-plot, the safe working fatigue stresses will be obtained, for a wide range of crack sizes "non-propagating cracks", as presented by the dashed area in the plot. However, it is necessary to compare these results with similar data in similar materials. Unfortunately such data are not available and, also, very sparse. The majority of published data has been generated on aluminum alloys and steels (21-25) where the critical values are considerably different.

The log-log diagrams of Figure (9) depict the relationship between the crack propagation rate per cycle da/dN and stress intensity factor range ,ΔK, from the steady state crack growth, to the threshold region for both the PDI and FDI. Fatigue crack growth rates for DI_s are generally higher than for most steels (2,21 and22); this may be ascribed to the effect of spheroidal graphite, which are considered to cause a reduction in the net section and Young's modules than those of steels, thus leading to higher crack growth rates. On the other hand, the relatively lower crack growth rate, obtained in FDI is attributed to the fracture mechanisms involved in the propagation process. The typical mechanism of fatigue crack propagation in ferritic matrix is associated with striation formation, which involves a minimum value of crack growth rate (the striation spacing distance) (3,18and 35). Whereas, in PDI micro cleavage mostly occurs in the pearlitic structures, in addition to the striation formation in the ferritic ring, surrounding graphite nodules. Therefore, a resultant higher crack propagation rate was obtained. The relatively higher threshold of stress intensity factor, obtained in PDI is attributed to the inherent higher resistance of pearlitic structure, especially in the range of non-propagating cracks. Since DI_s have lower Young's modules smaller than steels, therefore, it was expected that the threshold stress intensity factor ΔK_{th} to be smaller than steels, however, larger values of ΔK_{th} were obtained. These results are in good agreement with those obtained by other investigators (7,36 and 37). This may suggests that spheroidal graphite plays an important role in the near-threshold crack growth behaviour, which needs a more extended work, especially the role of graphite nodules in the crack closure .

Figures (11) and (12) indicate the relationship between the applied stress range $\Delta\sigma$ multiplied by the shape factor Y or ($Y.\Delta\sigma$) and the initial flow size,a_i, at definite fatigue lives for PDI and FDI respectively. These curves showed the influence of pre-existing sharp defects on the fatigue life of large section DI components. If the applied stress-initial flaw size combination falls on or above the single cycle fracture line (described by the plane strain fracture toughness K_{1c} values), then fracture can be expected to occur on the first loading. If, for a particular situation, the applied stress-initial flaw size falls below this line, then the component has a finite cyclic life. The effect of stress value ($Y.\Delta\sigma$) becomes pronounced as the difference between initial flaw size and critical flaw size increased.

The advantage of this type of plot is that it shows, for large section components, both single cycle data as well as cyclic data. Moreover, as non-destructive testing techniques are refined so as to estimate subsurface initial flaw size, before a component goes into service, then, by knowing cyclic stress, one can closely estimate cyclic life and determine if design requirements will be met or not. If not, the diagram can show what minimum flaw size is required and hence assists in determining the appropriate non-destructive testing technique that should be used to reliably detect that flaw size.

Further analysis of the results indicated that, far greater cyclic life can be realized by decreasing initial flaw size than by increasing the plane strain fracture toughness, via material modifications. Thus, it may be concluded that plane strain fracture toughness has a second-order effect on cyclic life. Moreover, the use of FDI provides longer fatigue lives, as ferritic matrix can tolerate the critical defect size to a greater extent.

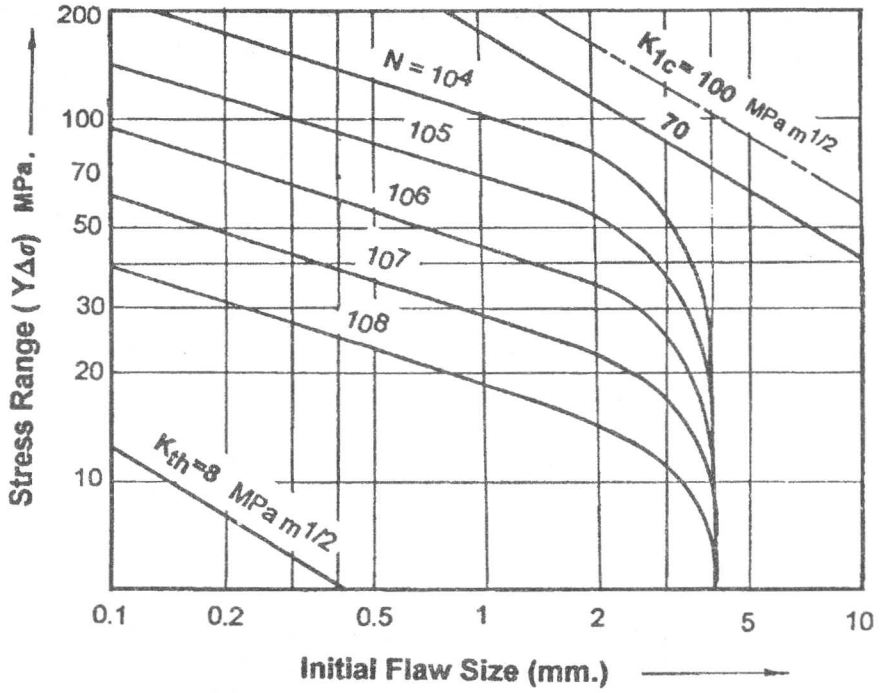

Figure 11. Fatigue life prediction for pearlitic DI containing initial defects.

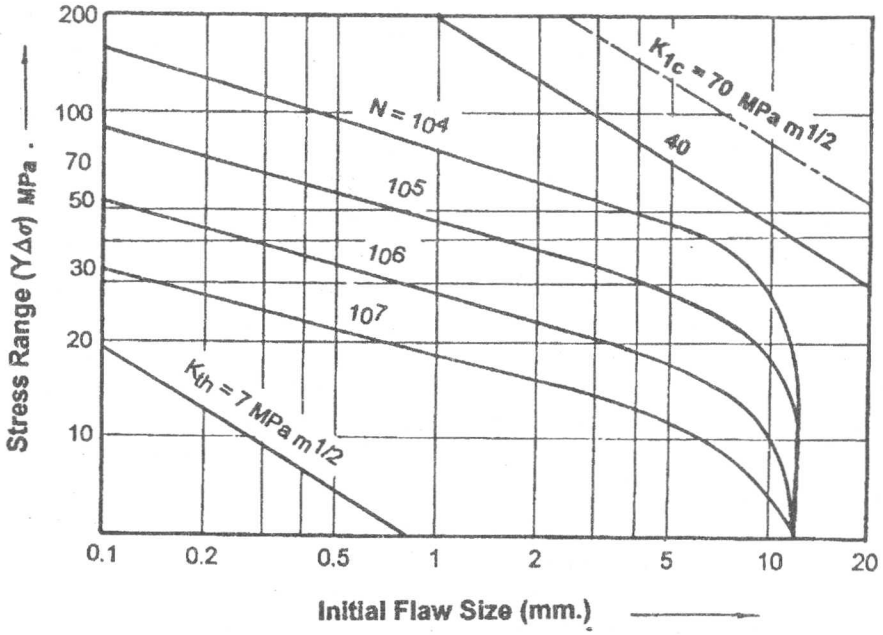

Figure 12. Fatigue life prediction for pearlitic DI containing initial defects.

CONCLUSIONS

(1) Size of metallurgical defects is considered to represent a lower bound of surface roughness; as fatigue cracks originated from these points, c to the inherently three-dimensional nature. Su defects responsible for crack initiation are i order of or greater than the maximum si

present metallurgical defects. Improving the quality of the surface by super-finishing processes, will not have a measurable effect on the bending fatigue life of DI.

(2) For these grades of DI, with a stress ratio R=-1; surface defects smaller than 100 μm would have little or no effect on the bending fatigue strength. Beyond 250 μm defect size, the fatigue strength of PDI has shown to decrease with increasing severity of surface roughness and, at notch depth of $R_{max} > 1.5$ mm. LEFM predictions become too conservative.

(3) The relatively higher crack growth rate da/dN, obtained for PDI is attributed to the micro cleavage fracture morphology associated with pearlitic structure. Whereas, striation formation in ferritic structure which involves a minimum value of crack propagation results in a lower crack growth rate.

(4) For large section components, greater cyclic life can be obtained by decreasing initial flaw size than by increasing plane strain fracture toughness. Moreover, the use of FDI provides longer fatigue life, as ferritic matrix can decrease the crack growth rate and tolerate the critical defect size to a greater extent. The inspection and control of defect size is of high importance, in order to guarantee safety and reliability of machine components subjected to fatigue .

ACKNOWLEDGMENTS

The author would like to acknowledge Eng. K. Abd-Ehamid and Eng. M. Eid for their pioneering work in constructing the push-pull fatigue testing machine as a B.Sc. Project. The help offered by Egyptian Iron and Steel Company and Helwan Company for Machine Tool Equipment in providing raw materials and manufacturing facilities is highly appreciated. The support of Helwan Iron Foundries and Benha higher Polytechnic Institute is gratefully acknowledged. Considerable assistance was provided by Eng. A. E. Attia and S. Laban in the fatigue tests as B.Sc. Projects.

REFERENCES

[1] D. Taylor and O.M.Clancy: "The fatigue performance of machined surfaces". Fatigue of Engineering Materials. 1991 vol.(14), pp.329-336.

[2] P.Greenfield and D.H.Allen:" The effect of surface finish on the high cycle fatigue strength of materials. GEC Journal of Research. 1987 vol.5, pp.129-140.

[3] M.Castagna et al:"Fatigue properties of in-mold ductile iron", AFS Transactions. 1978, pp 573-582.

[4] A.G.Fuller:" Effect of graphite form on fatigue properties of pearlitic ductile irons", AFS Transactions. 1977, pp. 527-536.

[5] "Deformation and Fracture Mechanics of Engineering Materials", Richard W.Hertzberg, second eddition. John wiley & sons. New York.

[6] P. Lukáš et al: "Notch size effect in fatigue", Fatigue of Engineering Materials. 1989 vol.12, pp. 175-186.

[7] P.Clemant et al: "Short crack behaviour in nodular cast iron". Fatigue of Eng. mat. vol.7, pp. 251-265.

[8] K.J.Miller:" The behaviour of short fatigue cracks and their initiation". Part I, and part II. Fatigue of Eng.Mat. 1987 vol.10, pp. 75-91 and pp. 93-113.

[9] Progress in Flaw Growth and Fracture Toughness Testing. Proceedings of the 1972 National Symposium on Fracture Mechanics. ASTM Special Technical Publication. Philadelphia.

[10] K.S.Chan and J.Lankford:" The role of microstructural dissimilitude in fatigue and frcture of small cracks". Acta metallurgica-1988 vol.36, pp.193-206.

[11] Zuyu Sun et al: "Modeling Small fatigue cracks interacting with grain boundaries". Fatigue of Eng. Mat. 1991 vol. 14 pp. 277-291.

[12] M.H.El-Haddad: "Fatigue life predictions of smooth and notched specimens based on fracture mechnics", Transactions of the ASME, Journal of Engineering Materials and Technology, 1979. vol.101, pp.91-96.

[13] M.H.El-Haddad et al:" Fatigue crack

propagation of short cracks". Transactions of the ASME, Journal of Engineering Materials and Technology 1979. vol.101, pp. 42-45.

[14] Tao Ye et al: "Effect of notch stress field and crack closure on short fatigue crack growth" Fatigue of Eng. Mat. 1990 vol. 13 pp. 423-430.

[15] Keiro Tokaji and Takeshi Ogawa :"Small fatigue crack growth in a low carbon steel under tension-compression and pulsating- tension loading" Fatigue of Eng. Mat. 1990 vol. 13 pp. 31-39.

[16] Keiro Tokaji et al:" Evaluation on limitation of linear elastic fracture mechanics for small fatigue crack growth". Fatigue of Eng. Mat.1987. vol.10, pp. 281-289.

[17] Keiro Tokaji et al: "Limitations of linear elastic fracture mechanics in respect of samall fatigue cracks and microstructure". Fat. of Eng. Mat.1986.vol.9, pp.1-14.

[18] S. Majumdar and P.S.Maiya:"A mechanistic model for time-dependent fatigue short cracks" Transactions of the ASME", journal of Engineering Materials and Technology. 1980 vol.102, pp. 159-167.

[19] K.H.Schwalbe et al:" Draft EGF recommendations for determining the fracture resistance of ductile materials: EGF procedure EGF P1-87D. Fatigue of Eng. Mat. 1988 vol.11,pp. 409-420.

[20] B.K.Neale and E.K.Priddle:" On fatigue crack growth and stabl tearing". Fatigue of Eng. Mat. 1988 vol.11, pp. 31-43.

[21] E.K.Priddle:" The influence of test variables on the fatigue crack growth threshold". Fatigue of Eng. Mat. 1989 vol. 12, pp. 333-345.

[22] R.O.Rilchie: "Near-threshold fatigue crack propagation in Ultra-high strength steel: influence of load ratio and cyclic strength" Transactions of the ASME, J. of Eng. Mat.and Tech. Joly 1977, pp.195-204.

[23] T.T.Shih and J.K.Donald:" Threshold and low-rate fatigue crack growth of a NiMoV rotor steel". Transactions of the ASME, J.of Eng. Mat. and Tech.vol.103. 1981, pp. 104-111.

[24] Shihji Kumaa et al:" Short and long fatigue crack growth in a Sic reiforced aluminium alloy ". Fatigue of Eng. Mat. 1990. vol.13, 511-524.

[25] M.J.Couper and J.R.Griffiths: "Effect of closure and mean stress on the threshold intensity factor for fatigue of and alum casting alloy". Fatigue of Eng. Mat. vol.13, pp. 615-624.

[26] R.J. Allen et al: "A review of fatigue growth characterization by linear elastic fr mechanics (LEFM)". Part I and part II. F of Eng. Mat.1988. vol.11, pp. 45-69 71-108.

[27] Yozo Sawaki et al: "Fatigue fracture tou and crack propagation rate". Interna Journal of Fracture 1987. vol.35, pp. 12

[28] R.H.Sailors:" Presentation of failure an data by fatigue fracture mechanics diag Transations of the ASME 1987, pp.673-6

[29] F.S. Ahmed:" Influence of heat treatme mechanical properties of austempered iron ". The Egyptian Foundrymen Soc. Magazine 1992. vol. 48, pp. 27-39.

[30] F.S. Ahmed: "Improving the bending stregth of ductile cast iron " The Eg Foundymen Soc. Magasine 1993 vol. 50 31-52.

[31] Standard test method for measurement of crack growth rates E-647-88. ASTM book of standards.

[32] Standard practice for statistical analysis of or linearized stress-life (S-N) and stra (F-N). Fatigue data E 739-(80). ASTM book of standards pp. 655-661.

[33] F.S.Ahmed and Ahmed A. El-Zo "Fracture toughness of nodular and verm cast iron". The Egyptian Foundrymen Magazine Sept. 1988.

[34] F.S.Ahmed et al:" Fracture toughne austempered ductile iron The Eg Foundrymen Soc. Magazine 1993. Vol 51 20.

[35] J.Pokluda and J.Siegl:" Mixed fatigue fr morphology of ferritic ductile iron" Fatig Eng. Mat. 1990 vol. 13 pp. 375-385.

[36] Takashi et al: "Near-threshold fatigue growth and crack closure in a nodular cast Fatigue of Eng. Mat. 1987 vol. 10 pp. 27

[37] A.J.Krasowsky et al:" Fracture toughness of nodular graphite irons under static impact and cyclic loading "Fatigue of Eng. Mat. 1987 vol. 10 pp. 223-237.

[38] A Push-Pull fatigue testing machine for high cycle tests. M. Zaky. MSc Thesis-Cairo Univ. Faculty of Eng. Mech. Design and Production Department.

Appendix

The Figure shows a schematic sketch showing the main idea of the machine, in which a rigid frame(1), made to support the housing of the loading system and suspend the upper specimen grip (2). The lower grip (3) is bolted to the loading end of a heavy duty tension-compression spring (4). Displacement of the lower spring seat is adjusted by means of a horizontal lever (5), actuated with a came (6) to control the stress amplitude of the moving seat. Mean load is applied by turning a nut (7), attached with worm and gear unit (8) to provide sensitive and controlled motion of the power screw (9), this raises the upper grip; stressing the suspension system of the loading seat (ref.38). Both static and cyclic loadings are measured using a load cell (10) arranged at the lower end of power screw and connected to a strain bridge. The machine was statically calibrated using dead weights. In order to ensure stress cycle, an oscilloscope is used during dynamic calibration. The number of cycles were recorded using digital counter (11). The crack length was measured by using a calibrated low power traveling microscope mounted in micrometer slide, this enables crack growth increments of 0.1mm to be measured.

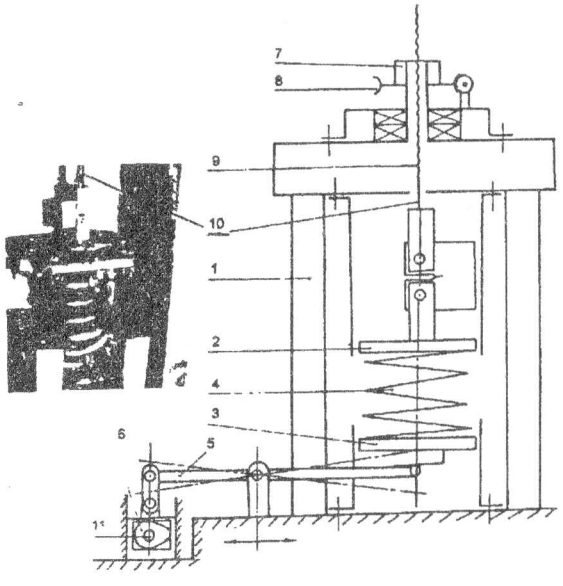

Schematic of fatigue setup .